FUTURE PROJECTION OF OCEAN WAVE CLIMATE CHANGE USING MULTI-SST ENSEMBLE EXPERIMENTS

Tomoya Shimura[1], Nobuhito Mori[2],Tomohiro Yasuda[2] and Hajime Mase[2]

Long term changes in ocean waves elicit a variety of impacts on a coastal environment. In order to assess the future changes in ocean wave climate, future projections of global wave climates have been carried out by previous studies. However, previously there has been little discussion about the causes behind changes in future wave climate and the differences between projections. The objective of this study is to estimate the future changes in mean wave climate and the sensitivity of the wave climate to Sea Surface Temperature (SST) conditions, in an effort to understand the mechanism behind the wave climate changes by specifically looking at spatial SST variation. A series of wave climate projections forced by surface winds from the MRI-AGCM3.2H were conducted based on SST ensemble experiments. The results show future changes in seasonal mean wave heights that are within about ± 0.4 m depending on the region and season. The future changes in summertime wave heights in the Western North Pacific (WNP) are highly sensitive to SST conditions that are influenced by tropical cyclone changes. The spatial variation of SST in the tropical Pacific Ocean is a major factor in the wave climate changes for the WNP during summer.

Keywords: climate change; wave climate; future projection

INTRODUCTION

The number of studies assessing the impacts of long-term change in oceanographic phenomena related to climate change has been increasing (e.g., Hallegatte et al., 2013). Long term changes in ocean surface gravity waves produce impacts for a variety of disciplines. Ocean waves are one of the key components of beach morphology (Short, 1999), and wave energy may be a promising renewable energy source (Cruz, 2008). Changes in long term wave climates have been observed by voluntary observing ships (Gulev and Grigorieva, 2004), reanalysis data (e.g. Wang and Swail, 2001, Semedo et al., 2011), satellite imagery (Hemer et al., 2010, Young et al., 2011) and buoy data (e.g. Menéndez et al., 2008). Impacts of long term wave climate variability and change have been also reported. Kuriyama et al. (2012) found that, for a span of 22 years, the inter-annual shoreline variation at the Japanese coast has been induced by the fluctuation of the deep water wave energy flux. Sasaki (2012) estimated climatological annual mean wave energy around Japan based on 30 years of observations and found an increasing trend caused by more frequent swells. Furthermore, wave inundation has occurred across the western tropical Pacific, and recent accelerated sea level rise contributed to the severity of the impact (Hoeke et al., 2013).

A few studies have assessed impacts of future changes in wave climate using future wave climate projections under greenhouse gas emission scenarios. For example, Suh et al. (2012) examined the impact of climate change on a caisson type breakwater, including the effect of changes in wave height at the end of this century. Charles et al. (2012) has projected future wave climates for the Bay of Biscay and concluded that changes in wave conditions are leading to a decrease in the annual net longshore drift. The quantitative projection of future wave climates, including the likely range expected, is information that would be very useful to assess coastal impacts and how coastal communities will need to adapt.

To assess the future change in wave climate, several future projections of global wave climate have been conducted using different forcing mechanisms and wave models (Mori et al., 2010; Dobrynin et al., 2012; Hemer et al., 2013b; Fan et al., 2013; Semedo et al., 2013) and statistical models (Wang and Swail, 2006; Mori et al., 2013). Consequently, multi-model ensemble projections of global wave climate have been carried out in the Coordinated Ocean Wave Climate Project (COWCLIP, Hemer et al., 2012, 2013a; IPCC-AR5, 2013). The results of five independent studies (Wang and Swail, 2006; Mori et al., 2010; Hemer et al., 2013b; Fan et al., 2013; Semedo et al., 2013) showed a consistent future change in mean wave climate among models: future increases in wave height over the Southern Ocean, and decreases in wave height in the subtropics (Hemer et al., 2013a). However, there is little discussion about the cause of changes in future wave climate and the differences between models. Confidence with the projection is greatest if we understand the relationship between external forcing and the physical processes (Knutti et al., 2013).

A dynamical approach of global wave projection has been developed over the last few years (Mori et al., 2010; Hemer et al., 2013b; Fan et al., 2013; Semedo et al., 2013), and this approach is employed by this study. A framework of the approach can be described as follows.

[1]Graduate School of Engineering, Kyoto University, Japan
[2]Disaster Prevention Research Institute, Kyoto University, Japan

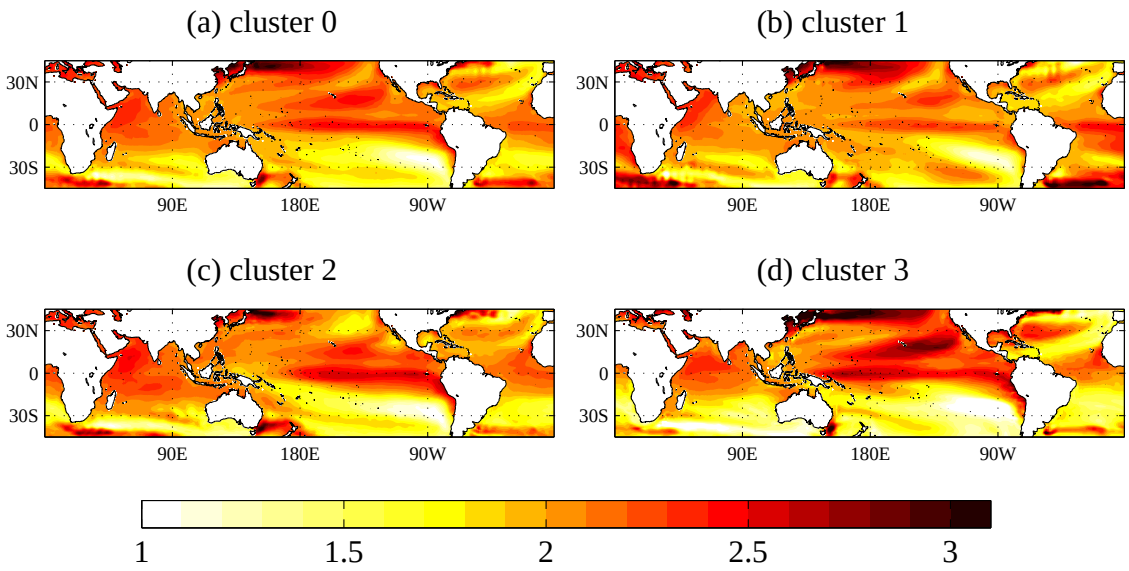

Figure 1: Future changes in annual mean SST for the case of (a) cluster 0, (b) cluster 1, (c) cluster 2 and (d) cluster 3 (unit:°C)

(1) Global climate simulation by an Atmosphere-Ocean Coupled General Circulation Model (AOGCM) under an emission scenario.

(2) Global atmospheric climate simulation by an Atmospheric GCM (AGCM) using Sea Surface Temperature (SST) data from the AOGCM as a boundary condition.

(3) Global wave simulation by a wave model forced with the sea surface winds of the AGCM.

The procedure in item (2) is sometimes skipped (Dobrynin et al., 2012), but the climate projection with an AGCM is useful for impact assessments because the AGCM has a finer spatial resolution over the AOGCM, with lengths in the range of 20 to 100 km, generally.

The choice of SST is arbitrary for the AGCM; ensemble mean SST of several AOGCMs is sometimes used for a simulation. SST, however, can lead to a fundamental variation in the general circulation and yield significant impacts on the wave climate projection through the sea surface winds. Therefore, it is important to estimate the sensitivity of a wave climate projection to projected SST. The objective of this study is to estimate the response and the sensitivity of mean wave climates to projected SST. A series of wave climate projections using the same AGCM are conducted based on SST ensemble experiments. First, this study shows the response and the sensitivity of seasonal mean wave heights to projected SST conditions quantitatively, indicating that future summer wave heights in the Western North Pacific (WNP) are sensitive to SST conditions. Second, climatological causes behind future wave climate change in the WNP are discussed in detail with typhoons. In order to generalize the results, we consider the perturbed physics (PP) ensemble experiments in addition to SST ensemble experiments.

METHODOLOGY

The framework of wave climate projection of this study is same as that described in the Introduction section. First, the methodology of atmospheric climate projection by AGCM using SST projected by AOGCM as the boundary condition, is described. Next, the methodology of wave climate projection by wave model forced by sea surface wind of AGCM, is described.

Atmospheric climate projection

The AGCM used in this study was developed by the Japanese Meteorological Research Institute, the so-called MRI-AGCM version 3.2 (denoted as MRI-AGCM3.2, Mizuta et al., 2012) for IPCC-AR5 (2013). The SST and perturbed physics ensemble experiments were carried out with the 60 km horizontal spatial

resolution model of MRI-AGCM3.2 which is denoted as MRI-AGCM3.2H, and the results of the MRI-AGCM3.2H were used for this analysis. The forcing to AGCM is SST, sea ice at the bottom boundary and green house gases in the atmosphere.

The time slice experiments were conducted using 1979 to 2009 for the present climate and 2075 to 2099 for the future climate, respectively. Lower boundary conditions of MRI-AGCM3.2H in the present climate were monthly mean observed sea ice concentration and SST from the Hadley Centre Global Sea Ice and Sea Surface Temperature dataset (HadISST1; Rayner et al. 2003). The boundary conditions for the future climate consisted of four different statistically analyzed SSTs (Murakami et al., 2012). The four future SST conditions as boundary conditions of MRI-AGCM3.2H were defined based on SST projected by eighteen models of the Coupled Model Intercomparison Project Phase 3 (CMIP3, Meehl et al., 2007). The first SST condition is the ensemble mean SST projected by eighteen models of CMIP3 under A1B scenario of the Special Report on Emission Scenarios (SRES). The other three future long-term SST trends are differently classified future SST patterns derived by cluster analysis of the future change pattern of SST from eighteen CMIP3 models under the A1B emission scenario. The detail of the clustering analysis of future SST conditions was described in Murakami et al. (2012). Interannual variations of the future climate SST are given by detrended interannual variations of present climate SST (1979-2003), based on the assumption that the interannual variations of SST in the future climate are similar to those of the present climate.

The four different SSTs are denoted as clusters 0 to 3, where cluster 0 means the mean of the eighteen CMIP3 models. **Figure** 1 shows future changes in SST for clusters 0 to 3. All the SST patterns show that SST in the future climate increases over most of the entire ocean, with increases up to about 3 °C. The North Pacific, especially, shows a greater increase in temperature than any other region. The different clusters of SST show different spatial characteristics. Cluster 3 shows the warmest SST and cluster 1 shows the lowest SST in the tropical Pacific. Cluster 2 shows the warmest SST in the tropical Indian Ocean. The spatial standard deviations of temperature rise in the tropics (30°S to 30°N) are 0.24, 0.21, 0.27, 0.38 °C for cluster 0 to 3, respectively. Fan et al. (2013) and Hemer et al. (2013b) also conducted global wave climate projections based on several SSTs. SSTs in Fan et al. (2013) and Hemer et al. (2013b) were derived from arbitrary CMIP3 models. On the other hand, four SSTs in this study can objectively express the representative SSTs of eighteen CMIP3 models because of the cluster analysis.

The PP ensemble experiments were conducted with three different cumulus convection schemes: Yoshi mura (YS), prognostic Arakawa-Schubert (AS) and the Kain-Fritsch (KF) scheme (see detail in Murakami et al., 2012). The target of PP ensemble experiments was sensitivity of cumulus convection scheme to tropical cyclone projection. It will be discussed the later part of this manuscript.

Wave climate projection

Global wave climate projection was carried out by WAVEWATCH III version 3.14 (Tolman, 2009) forced by sea surface wind from MRI-AGCM3.2H. WAVEWATCH III has been used for hindcast, nowcast and future global wave projection studies (Hemer et al., 2013b; Fan et al., 2013). The global domain was set for the latitudinal range of 90°S-67°N over all longitudes with $1° \times 1°$ spatial grids. Directional resolution is 15°, and the frequency space is 0.04 to 0.5 Hz, which is discretized in 25 increments logarithmically as a conventional setup. The Tolman and Chalikov (1996) source term package was used as a set for wind input and dissipation. WAVEWATCH III can represent unresolved islands (Tolman, 2009). The nesting in the WNP (11°N-50°N and 121°E-160°E) was performed with 0.5° spatial resolution and 10° directional resolution. Sea ice was not considered in this wave climate simulation. The model performance of wave climate was shown compared with reanalysis data set and buoy observations by Shimura et al. (2014).

Ensemble experiments of wave climate projection were organized as three present climate experiments based on the three PP ensemble experiments and twelve future climate experiments based on three PP ensemble experiments and four SST ensemble experiments. However, at first, the results of the SST ensemble experiments with only YS cumulus convection schemes are shown in order to focus on the effect of SST differences. And then, in the discussion of wave climate in WNP, the results of PP ensemble experiments are shown in order to estimate the effect of SST differences relative to perturbed physics. The climate simulation for the present climate condition is denoted as HPA and those for future climate conditions with SST clusters 0 to 3 are denoted HFAc0, HFAc1, HFAc2, HFAc3, respectively for simplicity.

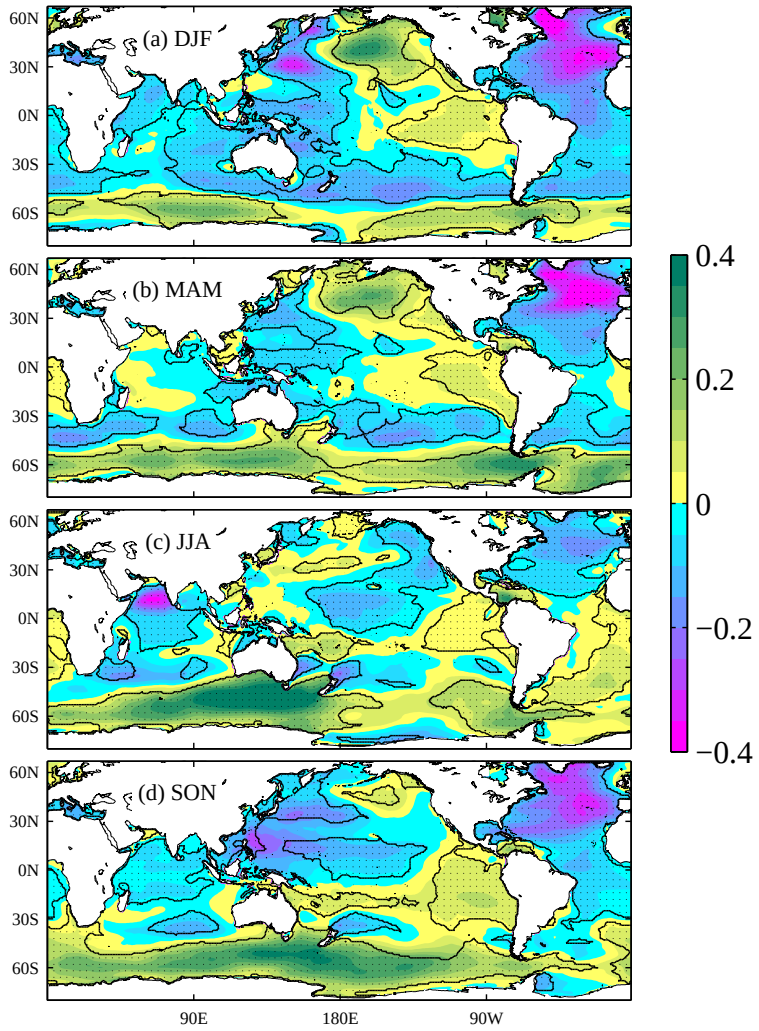

Figure 2: Future changes in MSWH during (a) DJF, (b) MAM, (c) JJA and (d) SON (unit:m). Regions with black dots indicate areas where the four future projections of HFAc0 to HFAc3 show the same sign.

FUTURE CHANGES IN GLOBAL WAVE CLIMATE : MSWH

This section looks at future changes in MSWH on the global scale during all four seasons and the sensitivity of MSWH to SST conditions. The four seasons are classified as December to February (DJF), March to May (MAM), June to August (JJA) and September to November (SON). **Figure** 2 and **Figure** 3 show the ensemble mean and maximum differences of future changes in MSWH as $\sum_{i=0}^{3}$(HFAc*i*-HPA)/4 and $\max_{i=0,1,2,3}$(HFAc*i*-HPA) - $\min_{i=0,1,2,3}$(HFAc*i*-HPA). In the figure, the black contoured regions with dots indicate the regions where future changes of HFAc0 through HFAc3 show the same signs (positive or negative) for reliability of projections. In regions where future changes of HFAc0 through HFAc3 show both different signs and larger differences, these areas have large uncertainty in the projected wave height, which is related to the uncertainty in SST condition. Future changes in MSWH are about -0.4 to +0.4 m depending on the region and the season, and the maximum differences are up to about 0.4 m. Therefore, the uncertainty of the MSWH projection has the same magnitude as its future change.

DJF

The wave heights increase (˜0.4 m) in the central mid-latitudes of the North Pacific and decrease in the WNP around 30°N (**Figure** 2(a)). Notable decreases (-0.4 m˜) are shown in the North Atlantic, and

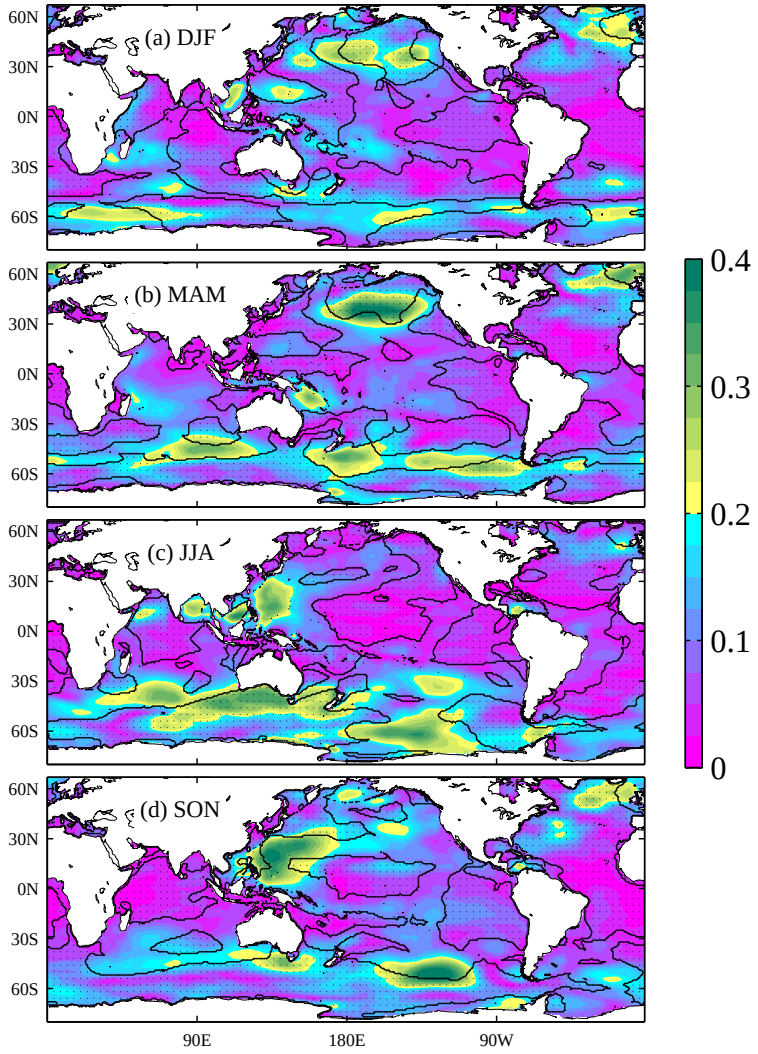

Figure 3: Maximum differences in future change of MSWH during (a) DJF, (b) MAM, (c) JJA and (d) SON (unit:m)

future changes in the Southern Hemisphere are characterized by increases at higher latitudes and decreases at mid-latitude. The regions where the four future changes of HFAc0 through HFAc3 show the same sign comprise 66.8% of the whole domain. The regions where future changes of HFAc0 through HFAc3 show different signs and larger maximum differences are the lower latitudes of the WNP.

MAM

The spatial pattern of future change in MSWH during MAM is similar to that for DJF (**Figure** 2(a)(b)). The regions where the four future changes of HFAc0 through HFAc3 show the same sign comprise 58.6% of whole domain. Maximum differences of future change during MAM are larger than during DJF, especially in mid-latitudes of the North Pacific and northeast regions of the North Atlantic.

JJA

The future changes of MSWH during JJA are different than during DJF and MAM. The MSWH increases (˜0.5m) in the region 0°E-180°E of the Southern Ocean, and the MSWH decreases (-0.4m˜) in the Arabian Sea (**Figure** 2(c)). Regarding the uncertainty with the projections, the regions where the four future changes for HFAc0 to HFAc3 show same sign are 55.2% of whole domain. The regions with large maximum differences are located in the lower latitudes of the WNP, 30°S-40°S in the Indian Ocean and 60°S in the South Pacific (**Figure** 3(c)).

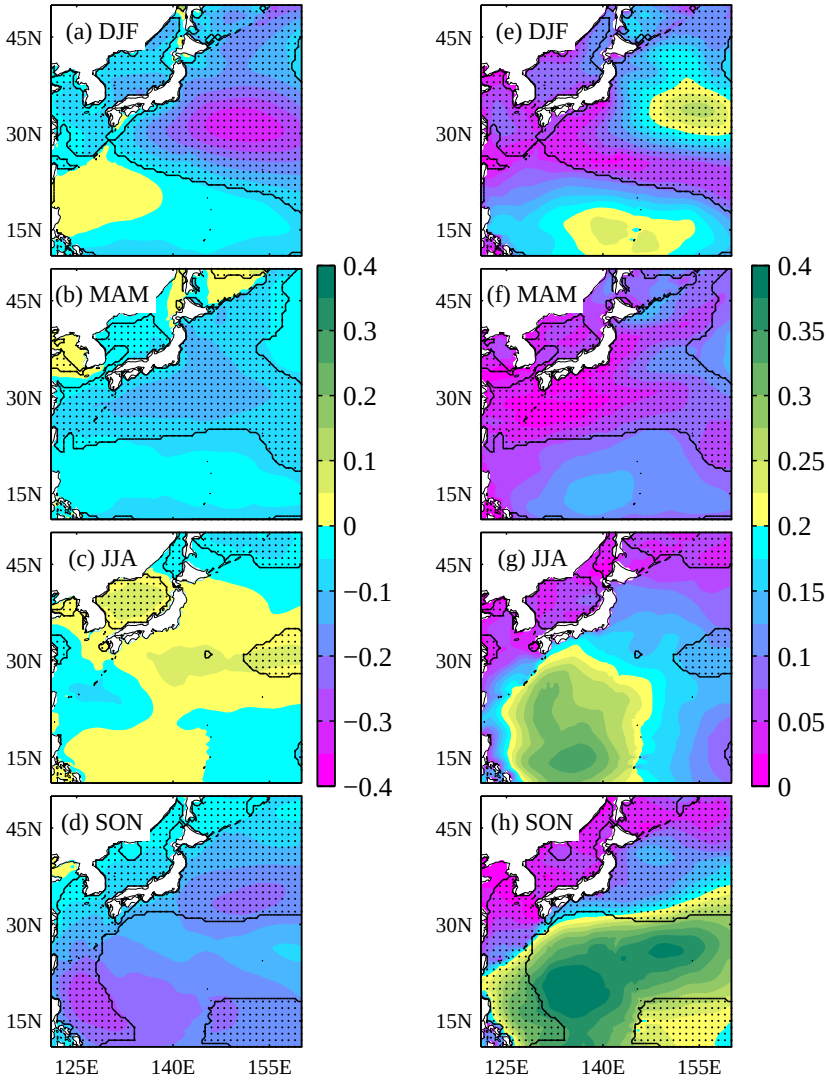

Figure 4: Future changes in MSWH for the WNP during (a) DJF, (b) MAM, (c) JJA and (d) SON, and the maximum differences in future change during (e) DJF, (f) MAM, (g) JJA and (h) SON (unit:m). Regions with black dots indicate areas where the four future projections show the same sign.

SON

Future changes of MSWH during SON can be characterized by decreases in the WNP and the North Atlantic, and increases in the Southern Ocean (60°S). The future change in MSWH is about ± 0.4 m on the global scale (**Figure** 2(d)). The regions where the four future projections by HFAc0 through HFAc3 show the same sign comprise 62.0% of whole domain. The regions where the future changes for HFAc0 to HFAc3 show different signs and larger differences are the lower latitudes of the WNP and the mid-latitudes of the South Pacific (**Figure** 3(d)).

As described in this section, the spatial patterns of future wave height changes differ depending on the season, and some regions exhibit relatively large uncertainty in projected wave heights depending on projected SST conditions.

FUTURE CHANGES IN WAVE CLIMATE FOR THE WESTERN NORTH PACIFIC

To discuss wave climate changes in the WNP in detail, the projected future changes of MSWH for the WNP, which were calculated by a nested 0.5°spatial resolution, are shown in this section. **Figure** 4 shows the future changes in MSWH and the maximum differences in the ensembles for the WNP. The

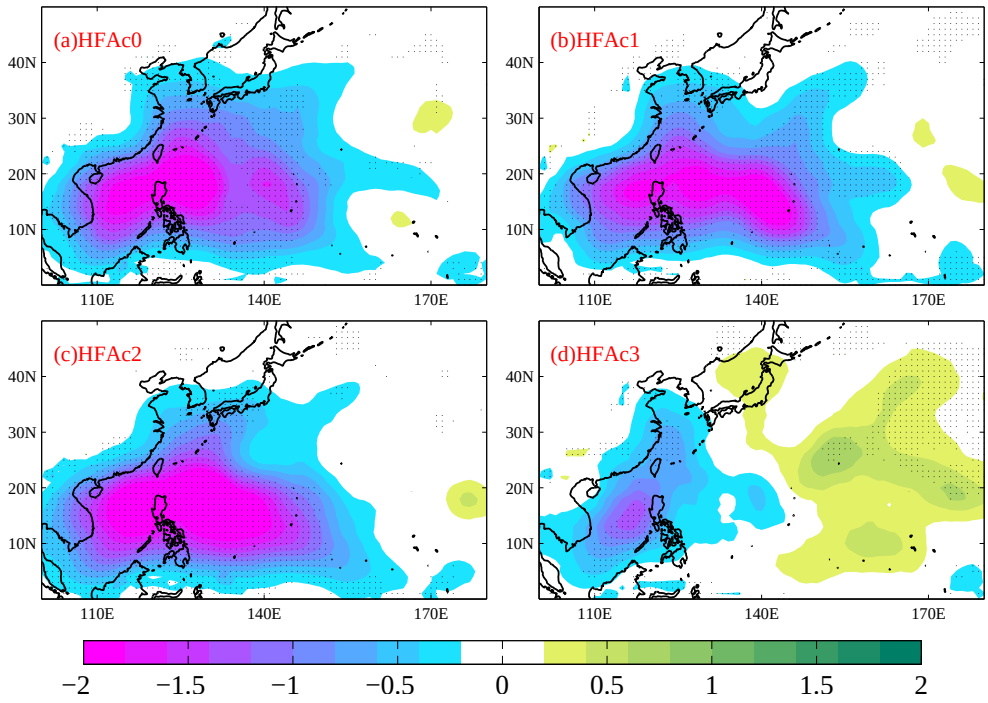

Figure 5: Future changes in the frequency of typhoon passing for (a)HFAc0, (b)HFAc1, (c)HFAc2 and (d)HFAc3. Regions with black dots indicate significant changes with 5% significance level tested by Mann-Whitney U test. (unit: #/season(JJASON))

biggest changes in the future wave climate can be seen around 30°N and 150°E during DJF, where the MSWH decrease is 0.3 m (**Figure** 4(a)). However, there are no significant changes of SWH during MAM and JJA (**Figure** 4(b)(c)). The future changes for HFAc0 to HFAc3 around the Japan coast show the same sign during all seasons except for JJA. During MAM, the values of the maximum differences in future change are the smallest. The uncertainty in the lower latitudes of 30°N during JJA and SON are larger. For example, the future changes in MSWH at 20°N-30°N and 130°E-150°E during SON are -0.24, -0.24, -0.23 and +0.07 m for HFAc0 to HFAc3, respectively. Although the results for HFAc0 to c2 are consistent each other, the future change of only HFAc3 is different. The seasons JJA and SON in the WNP are active typhoon seasons. Therefore, future changes in wave height and the large uncertainty in these seasons (JJA and SON) are discussed in relation to typhoon characteristics below.

The relationship between future changes in wave height and typhoon characteristics

The most active area of tropical cyclone over the globe is the WNP. We are going to focus on the analysis for JJA and SON jointly (JJASON) in the WNP to discuss typhoon effects hereafter. The typhoon data detected by Murakami et al. (2012) was used in this study. **Figure** 5 displays the future changes in typhoon frequency for HFAc0 to HFAc3. The results for HFAc0, HFAc1 and HFAc2 show less typhoon frequency in the active typhoon region. On the other hand, the reduction in typhoon frequency for HFAc3 is moderate compared with the other three experiments. As indicated above, the tendency of future SWH changes for HFAc3 is different to that of the other experiments. It can be considered that these differences of SWH change between HFAc3 and the other experiments are caused by the differences in future changes of typhoon frequency between the ensembles as shown by **Figure** 5. However the contributions of typhoon change to MSWH change are not quantitatively clear. Therefore, how changes in typhoon characteristics affect the MSWH was estimated quantitatively as follows. The total MSWH is represented as a combination of both typhoon and non-typhoon events.

$$\mathrm{MSWH} = \mathrm{MSWH_{tc}} \cdot r_{tc} + \mathrm{MSWH_{no}} \cdot (1 - r_{tc}) \tag{1}$$

where $\mathrm{MSWH_{tc}}$ is the MSWH under a typhoon condition (in other words, typhoon wave intensity), $\mathrm{MSWH_{no}}$ is the MSWH under a non-typhoon condition (non-typhoon wave intensity) and r_{tc} is the ratio for the period

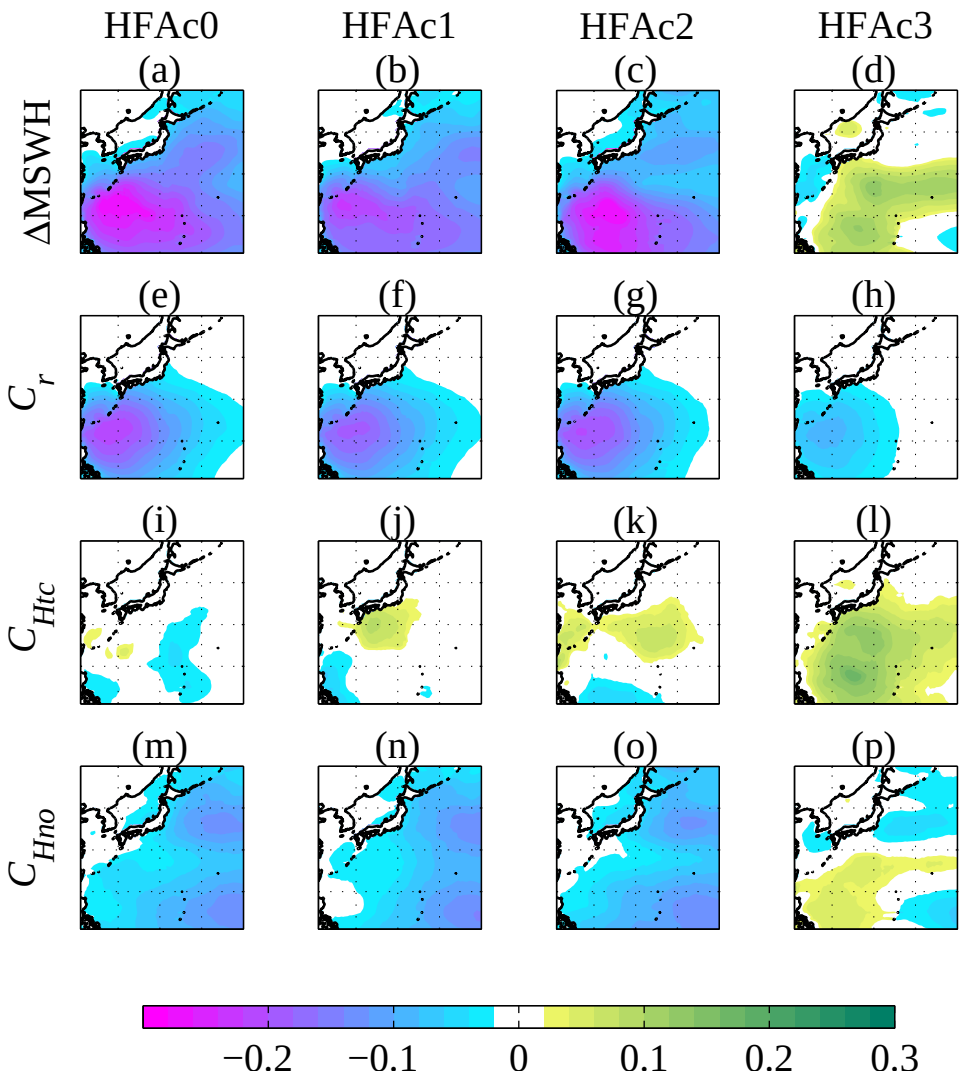

Figure 6: Future changes in MSWH in the WNP and the contributions of typhoon characterisitics changes (unit:m). Rows 1 to 4 show results for △MSWH, C_r, C_{Htc} and C_{Hno}. Columns 1 to 3 show results for HFAc0 to HFAc3.

of timeframe under a typhoon condition to the entire timeframe of the event (typhoon frequency). Eq. (1) can be rewritten for the future MSWH change (△MSWH) as

$$\begin{aligned} &\triangle\text{MSWH} \\ &= (\text{MSWH}_{\text{tc}} - \text{MSWH}_{\text{no}}) \cdot \triangle r_{tc} + \triangle\text{MSWH}_{\text{tc}} \cdot r_{tc} \\ &+ \triangle\text{MSWH}_{\text{no}} \cdot (1 - r_{tc}) + (\triangle\text{MSWH}_{\text{tc}} - \triangle\text{MSWH}_{\text{no}}) \cdot \triangle r_{tc} \\ &= C_r + C_{Htc} + C_{Hno} + C_{\triangle} \end{aligned} \tag{2}$$

where △ means future change, and C_r, C_{Htc}, C_{Hno} and $C_{\triangle}$ are contributions of $\triangle r_{tc}$ (typhoon frequency change), $\triangle\text{MSWH}_{\text{tc}}$ (typhoon wave intensity change), $\triangle\text{MSWH}_{\text{no}}$ (non-typhoon wave intencity change) and the residual to △MSWH. **Figure** 6 shows △MSWH, C_r, C_{Htc}, and C_{Hno} for HFAc0 to HFAc3. The figure clearly shows that △MSWH for HFAc3 is different from the other experiments (**Figure** 6(a) to (d)) as described above. The △MSWH for HFAc0 to HFAc2 shows decreases by 0.3 m, but for HFAc3 the value increases by 0.1 m. The value of C_r at lower latitudes is negative for all experiments due to a reduction in typhoon frequency in the future projection, but C_r for HFAc3 is relatively moderate compared to the others (**Figure** 6(e) to (h)), which follows the result of **Figure** 5. Furthermore, C_{Htc} for HFAc3 is larger

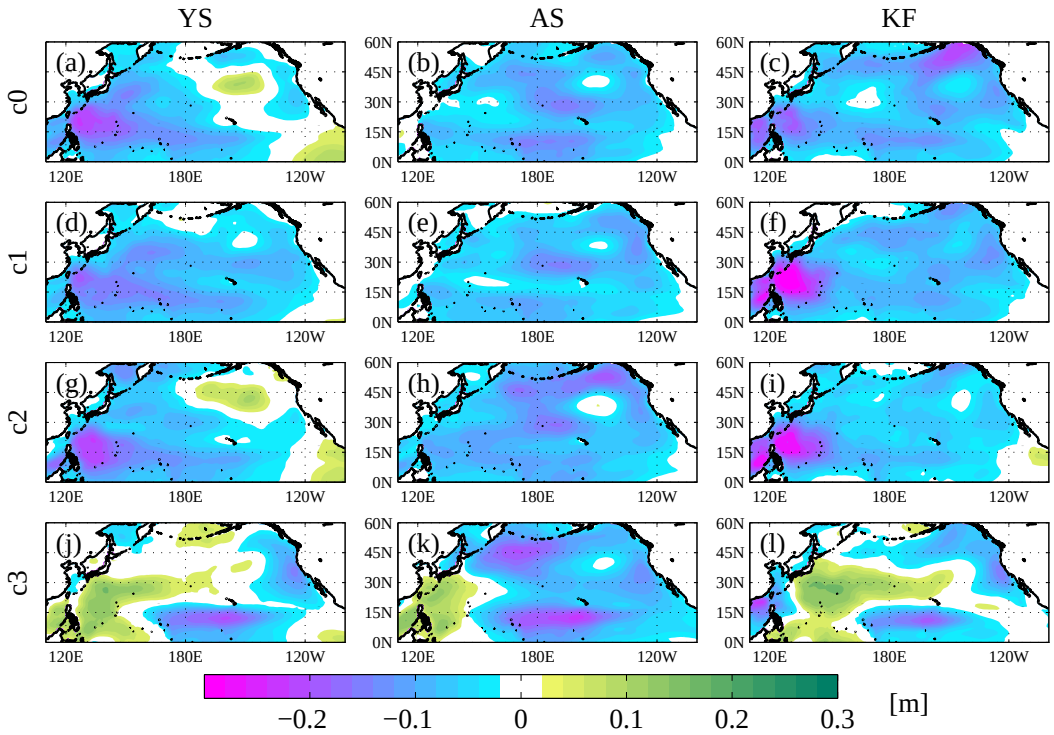

Figure 7: Future changes in MSWH during JJASON (unit:m). Rows 1 through 4 show results based on SST ensemble for cluster 0 through 3, from top to bottom. Columns 1 through 3 show perturbed physics ensemble results for YS, AS and KF schemes, from left to right.

than for the other experiments (**Figure** 6(i) to (l)). As a result, the differences in typhoon frequency (C_r) and typhoon wave intensity changes (C_{Htc}) between HFAc3 and HFAc0 to HFAc2 yield the differences in MSWH future change.

Comparison with PP ensemble experiments

The projections for MSWH by SST ensemble clearly illustrate the influence of tropical cyclones. In addition to SST ensemble projections, PP ensemble projections were conducted with three different cumulus convection schemes (YS, AS and KF). Note that the results shown in the above section are based on the YS scheme as described in Methodology section. In addition to SST ensemble experiments, PP ensemble experiments are included in this discussion. **Figure** 7 shows the future changes in MSWH based on the SST ensemble and PP ensemble, respectively. It is remarkable that future changes in MSWH from SST cluster 0 to 2 (**Figure** 7 except for (j)(k)(l)) are negative (-20% of present climate ∼) at lower latitudes (0-30° N) of the WNP. On the other hand, those under SST cluster 3 (**Figure** 7 (j)(k)(l)) indicate positive change in future projections (∼ +20%). PP ensemble exhibits less influence on differences of future change in MSWH in comparison with SST ensemble. There is a robust relationship between future patterns of SST and the summer wave climate in the WNP, such as the relative growth of mean wave height under SST cluster 3. It was found that this relationship can be seen in previous studies (COWCLIP: Mori et al., 2010; Hemer et al., 2013b; Fan et al., 2013; Semedo et al., 2013), although the detail of comparison with COWCLIP are omitted.

CONCLUSIONS

Future projections of global and WNP wave climate were conducted using the atmospheric global climate model (MRI-AGCM3.2H) and the wave model (WAVEWATCH III). In order to analyze the sensitivity of the projected wave climates to SST conditions, SST ensemble experiments were conducted. Four different future SST conditions (SST cluster 0 to 3) were used as boundary conditions for MRI-AGCM3.2H. The four SST conditions were defined based on SST projected by eighteen models of the Coupled Model

Intercomparison Project Phase 3 (CMIP3). One of the SST conditions is the ensemble mean SST of eighteen CMIP3 models, and the other three are representative SST conditions derived from eighteen CMIP3 models by applying cluster analysis to the future change patterns of SST.

Future changes in seasonal MSWH are about ± 0.4 m depending on the region and season. The regions where four future changes under four different SST conditions show the same sign covers 55 to 67% of the global domain depending on the season. Although some future changes are consistent with those from previous studies, such as increases in the Southern Ocean, and reductions during winter in the North Atlantic and 30°N of the WNP, some particular regions show either positive or negative future change depending on SST condition, a result that indicates the uncertainty of the future projection is large. The future changes in wave height in the WNP during the summer, where variation in future changes is large, were analyzed in detail. Future changes in MSWH for the lower latitudes of the WNP during the summer under SST cluster 3 are opposite in sign to those under the cluster 0 to cluster 2 conditions. Future changes under the SST cluster 3 condition are positive. The SST cluster 3 condition is characterized with higher warming in the equatorial Pacific (**Figure** 1).

The direct cause of these changes in future wave heights is future changes in the frequency and intensity of typhoons. This means that the variation in future changes of SST influences future changes in typhoon characteristics, and then that leads to differences in wave heights in the WNP. The results of PP ensemble experiments confirmed the relationship between the pattern for future change in SST and the wave climate in the WNP during the summer, such as the relative increase in the mean wave height under relatively warmer SST in the equatorial Pacific, namely the cluster 3 condition. Delcanbre et al. (2013) indicated that uncertainties in SST changes are a major source behind the Northern Hemisphere jet stream changes, suggesting that a reduction of uncertainty in the tropical Pacific SST response to global warming will significantly reduce uncertainty in the Northern Hemisphere zonal wind response to climate change. The same holds true for wave climate, especially in the WNP during the summer.

Although the details of the physical mechanism behind the relationship have not been addressed in this study, insight into what causes variations in wave projections can provide better understanding of ocean climate change. In this study, the cause behind variations in wave projections across SST conditions has been revealed, especially in the WNP. Knowing the future changes in wave climate can assist a wide variety of applications from beach morphology to engineering design.

ACKNOWLEDGEMENTS

Tomoya Shimura was supported by the Japan Society for the Promotion of Science (JSPS) Fellowships for Young Scientists and Grant-in-Aid for JSPS Fellows. This research was supported by the SOSEI Program Grant-in-Aid of the Ministry of Education, Culture, Sports, Science, and Technology (MEXT).

References

E. Charles, D. Idier, P. Delecluse, M. Déqué, and G. Le Cozannet. Climate change impact on waves in the Bay of Biscay, France. *Ocean Dynamics*, 62(6):831–848, 2012.

J. Cruz. *Ocean Wave Energy: Curent Status and Future Perspectives*. Springer-Verlag, Berlin, 2008.

S. C. Delcanbre, D. J. Lorenz, D. J. Vimont, and J. E. Martin. Diagnosing Northern Hemisphere jet portrayal in 17 CMIP3 global climate models: 21st century projections. *Journal of Climate*, 26:4930–4946, 2013.

M. Dobrynin, J. Murawski, and S. Yang. Evolution of the global wind wave climate in CMIP5 experiments. *Geophysical Research Letter*, 39:L18606, 2012.

Y. Fan, I. M. Held, S.-J. Lin, and X. L. Wang. Ocean warming effect on surface gravity wave climate change for the end of the 21st century. *Journal of Climate*, 26:6046–6066, 2013.

S. Gulev and V. Grigorieva. Last century changes in ocean wind wave height from global visual wave data. *Geophysical Research Letters*, 31:L24302, 2004.

S. Hallegatte, C. Green, R. J. Nicholls, and J. Corfee-Morlot. Future flood losses in major coastal cities. *Nature Climate Change*, 3:802–806, 2013.

M. Hemer, Y. Fan, N. Mori, A. Semedo, and X. Wang. Projected changes in wave climate from a multi-model ensemble. *Nature Climate Change*, 3:471–476, 2013a.

M. A. Hemer, J. A. Church, and J. R. Hunter. Variability and trends in the directional wave climate of the southern hemisphere. *International Journal of Climatology*, 30(4):475–491, 2010.

M. A. Hemer, J. Katzfey, and C. E. Trenham. Global dynamical projections of surface ocean wave climate for a future high greenhouse gas emission scenario. *Ocean Modelling*, 70:221–245, 2013b.

M. A. Hemer, X. L. Wang, R. Weisse, and V. R. Swail. Advancing wind-waves climate science: The COWCLIP project. *Bulletin of the American Meteorological Society*, 93(6):791–796, 2012.

R. K. Hoeke, K. L. McInnes, J. Kruger, R. McNaught, J. R. Hunter, and S. G. Smithers. Widespread inundation of pacific islands triggered by distant-source wind-waves. *Global and Planetary Change*, 108:128–138, 2013.

IPCC-AR5. *Climate Change 2013: The Physical Science Basis*. Cambridge Univ. Press, 2013.

R. Knutti, D. Masson, and A. Gettelman. Climate model genealogy: Generation CMIP5 and how we got there. *Geophysical Research Letter*, 40:1194–1199, 2013.

Y. Kuriyama, M. Banno, and T. Suzuki. Linkages among interannual variations of shoreline, wave and climate at hasaki, japan. *Geophysical Research Letters*, 39(6):L06604, 2012.

G. A. Meehl, C. Covey, K. E. Taylor, T. Delworth, R. J. Stouffer, M. Latif, B. McAvaney, and J. F. Mitchell. The WCRP CMIP3 multimodel dataset: A new era in climate change research. *Bulletin of the American Meteorological Society*, 88(9):1383–1394, 2007.

M. Menéndez, F. Méndez, I. Losada, and N. Graham. Variability of extreme wave heights in the northeast Pacific Ocean based on buoy measurements. *Geophysical Research Letters*, 35:L22607, 2008.

R. Mizuta, H. Yoshimura, H. Murakami, M. Matsueda, H. Endo, T. Ose, K. Kamiguchi, M. Hosaka, M. Sugi, S. Yukimoto, S. Kusunoki, and A. Kitoh. Climate simulations using MRI-AGCM3.2 with 20-km grid. *Journal of the Meteorological Society of Japan*, 90A:233–258, 2012.

N. Mori, T. Shimura, T. Yasuda, and H. Mase. Multi-model climate projections of ocean surface variables under different climate scenarios — Future change of waves, sea level and wind. *Ocean Engineering*, 71: 122–129, 2013.

N. Mori, T. Yasuda, H. Mase, T. Tom, and Y. Oku. Projection of extreme wave climate change under global warming. *Hydrological Research Letters*, 4(0):15–19, 2010.

H. Murakami, R. Mizuta, and E. Shindo. Future changes in tropical cyclone activity projectedby multi-physics and multi-SST ensemble experiments using the 60-km-mesh MRI-AGCM. *Climate Cynamics*, 39:2569–2584, 2012.

N. Rayner, D. Parker, E. Horton, C. Folland, L. Alexander, D. Rowell, E. Kent, and A. Kaplan. Global analyses of sea surface temperature, sea ice, and night marine air temperature since the late nineteenth century. *Journal of Geophysical Research: Atmospheres*, 108(D14):4407, 2003.

W. Sasaki. Changes in wave energy resources around Japan. *Geophysical Research Letter*, 39(L23702), 2012.

A. Semedo, K. Sušelj, A. Rutgersson, and A. Sterl. A global view on the wind sea and swell climate and variability from ERA-40. *Journal of Climate*, 24:1461–1479, 2011.

A. Semedo, R. Weisse, A. Behrens, A. Sterl, L. Bengtsson, and H. Günther. Projection of global wave climate change towards the end of the 21st century. *Journal of Climate*, 26:8269–8288, 2013.

T. Shimura, N. Mori, and H. Mase. Future projection of ocean wave climate : Analysis of SST impacts on wave climate changes in the Western North Pacific. *Journal of Climate, submitted*, 2014.

A. D. Short. *Handbook of beach and shoreface morphodynamics*. John Wiley & Sons, 1999.

K.-D. Suh, S.-W. Kim, N. Mori, and H. Mase. Effect of climate change on performance-based design of caisson breakwaters. *Journal of Waterway, Port, Coastal, and Ocean Engineering*, 138(3):215–225, 2012.

H. Tolman. User manual and system documentation of WAVEWATCH III version 3.14. *NOAA/NWS/NCEP/MMAB Technical Note*, 276, 2009.

H. L. Tolman and D. Chalikov. Source terms in a third-generation wind wave model. *Journal of Physical Oceanography*, 26(11):2497–2518, 1996.

X. Wang and V. Swail. Changes of extreme wave heights in Northern Hemisphere oceans and related atmospheric circulation regimes. *Journal of Climate*, 14(10):2204–2221, 2001.

X. Wang and V. Swail. Climate change signal and uncertainty in projections of ocean wave heights. *Climate Dynamics*, 26(2):109–126, 2006.

I. Young, S. Zieger, and A. Babanin. Global trends in wind speed and wave height. *Science*, 32:451–455, 2011.